α decay and spontaneous fission half-lives of nuclei around ^{270}Hs

C. I. Anghel[1,2] and I. Silişteanu[1,*]

[1]*Horia Hulubei National Institute of Physics and Nuclear Engineering, Bucharest-Magurele, 077125 Bucharest, Romania*

[2]*University of Bucharest, Faculty of Physics, 077125 Bucharest, Romania*

(Received 5 October 2016; revised manuscript received 8 December 2016; published 17 March 2017)

α decay and spontaneous fission half-lives of 81 superheavy nuclei with $Z = 104$–112 and $N = 158$–166 have been calculated with simple formulas extracted from the systematics of measured and calculated half-lives. Half-life calculations are performed within the shell model and one-body rate theories for α decay and a dynamical approach for spontaneous fission defined essentially by the shape, the height of fission barrier, the fissility, and the nuclear deformations. We obtained a rather good accordance between calculated and experimental half-lives for 30 nuclei with measured Q_α values. We predicted with different fitting formulas the most probable half-lives for 51 nuclides at which there are no experimental data. The rms values for experimental and theoretical half-lives are evaluated and discussed. The comparison of theoretical calculations with experimental data allows us to draw conclusions on the role of the nuclear structure and shell effects in low-energy decay processes.

DOI: 10.1103/PhysRevC.95.034611

I. INTRODUCTION

The search for α decay (AD) and spontaneous fission (SF) activities in the region of superheavy nuclei (SHN) started to emerge with cross sections and half-life measurements from several cross bombardments aimed at producing Rf isotopes [1–4]. More recently, experiments with improved reaction and detection techniques have been produced some isotopes of Rf, Db, Sg, Bh, Hs, Mt, Ds, Rg, and Cn elements [5–20]. The data on the properties of nuclear energy levels and decay modes of nuclei around ^{270}Hs show that the AD and SF are the most important and competing decay modes. Also, the AD data have been provided with theoretical support, some information on the single-particle states, the excitation energies of the daughter nucleus (fine structure), and level schemes of nuclei involved in AD transitions. The calculated ground state and decay properties of SHN [21–24] show a rather complex shell structure of well-deformed nuclei. Also, refined calculations [25–29] predicted large gaps in the single-particle energies for protons and neutrons at $Z = 108$ and $N = 152$ and 162 that provide added stability to deformed nuclei. The theoretical studies of SHN have been very intense in recent years. For AD half-lives there are estimates based on empirical relationships of Geiger-Nuttall type [30–33] and on the shell-model rate theory [34–40]. New approaches for obtaining information on the many-nucleon structure in α decay from accompanying bremsstrahlung emission and α-particle capture reactions were presented in recent papers [41–43]. Also the competition between SF and quasifission was analyzed in detail in Ref. [44]. The strong correlations between protons and neutrons near the Fermi surface define the shell stability line in asymmetric SHN [45]. Other correlations are connected with the symmetry energy [46]. The SF half-lives are estimated with an empirical formula derived from a dynamical approach for SF defined essentially by the shape, the height of fission barrier, the fissility, nuclear deformations [47], and even-odd corrections [48–50]. The competition between the AD and SF has been studied in a series of papers [50–54]. In this work, we analyze the available experimental data and the calculated nuclear decay properties of nuclei around ^{270}Hs with $Z = 104$–112 and $N = 158$–166. New half-life predictions are made for many unknown nuclei from this region. The paper is organized as follows. In Sec. II the theoretical formalism is briefly reviewed. The obtained results for the decay properties of SHN and the systematics of both AD and SF half-lives are presented in Sec. III. The concluding remarks are given in Sec. IV.

II. THEORETICAL FRAMEWORK

A. Shell model (SM) AD half-lives

First, we calculate AD half-life (of a decaying state k into a channel n) in the shell model rate theory [34,35],

$$T_n^k = (\hbar \ln 2)/\Gamma_n^k, \tag{1}$$

where the AD decay width is

$$\Gamma_n^k = 2\pi \left| \frac{\int_{r_{\min}}^{r_{\max}} I_n^k(r) u_n^0(r) dr}{\int_{r_{\min}}^{r_{\max}} I_n^k(r) u_n^k(r) dr} \right|^2. \tag{2}$$

In Eq. (2), $I_n^k(r)$ is the formation amplitude (FA) defined as the antisymmetrized projection of the parent wave function (WF) $|\Psi_k\rangle$ on the channel WF $|n\rangle = |[\Phi_D(\eta_1)\Phi_p(\eta_2)Y_{lm}(\hat{r})]_n\rangle$:

$$I_n^k(r) = r\langle \Psi_k | \mathcal{A}\{[\Phi_d(\eta_1)\Phi_\alpha(\eta_2)Y_{lm}(\hat{r})]_n\}\rangle, \tag{3}$$

where $\Phi_d(\eta_1)$ and $\Phi_\alpha(\eta_2)$ are the internal (space-spin) wave functions of the daughter nucleus and of the particle, $Y_{lm}(\hat{r})$ is the wave function of the angular motion, $\mathcal{A}$ is the interfragment antisymmetrizer, r connects the centers of mass of the fragments, and the symbol $\langle|\rangle$ means integration over the internal coordinates and angular coordinates of relative motion. The functions $u_n^{0,k}(r)$ in Eq. (2) represent the reaction amplitude (RA) and are the solutions of the system of differential

*silist@theory.nipne.ro

equations:

$$\left\{\frac{\hbar^2}{2M}\left[\frac{d^2}{dr^2}-\frac{l(l+1)}{r^2}\right]-V_{nn}(r)+Q_n\right\}u_n^0(r)+\sum_{m\neq n}V_{nm}(r)u_m^0(r)=0, \quad (4)$$

$$\left\{\frac{\hbar^2}{2M}\left[\frac{d^2}{dr^2}-\frac{l(l+1)}{r^2}\right]-V_{nn}(r)+Q_n\right\}u_n^k(r)+\sum_{m\neq n}V_{nm}(r)u_m^k(r)=I_n^k(r). \quad (5)$$

describing the radial motion of the fragments at large and small separations, respectively, in terms of the reduced mass of the system M, the reaction energy of emitted particle Q_n, the FA, and the matrix elements of interaction potential $V_{nm}(r)$. The matrix elements $V_{nm}(r)$ include nuclear and Coulomb components [35] defined with the quadrupole (β_2) and hexadecapole (β_4) deformation parameters of the daughter nucleus [47].

The use of shell-model rate theory (SMRT) needs the following:

(1) single-particle wave functions Ψ_k and Φ_d of the parent and daughter nuclei
(2) to calculate $I_n^k(r)$ we need to pass the four-nucleon wave function from individual coordinates r_i ($i=1-4$) to the center of mass and relative coordinates (r_1, r_2, r_3, r_4)$\rightarrow$ (r,ρ_1,ρ_2,ρ_3) and to integrate over relative spatial and angular coordinates [55]
(3) the search for eigenfunctions $[u_n^{0,k}(r)]$, eigenvalues (the resonance energy $Q_\alpha^{\rm res}$, the depth in origin of the Woods-Saxon nuclear potential $V_0^{\rm res}$), and the phase of the resonance scattering $\varphi^{\rm res}$ [56–58]; to avoid the usual ambiguities encountered in formulating the potential for the resonance tunneling of the barrier we iterate directly the depth in origin of the nuclear potential in the equations of motion
(4) the numerical integration of Eqs. (4) and (5) with boundary conditions.

We use in Sec. III C the SMRT results for AD half lives to obtain simple empirical relationships for half-life predictions.

B. One-body α-decay half-lives

Of particular importance to decay studies are the energy levels observed in fusion-evaporation reactions of heavy ions as very narrow α resonances that are measured via α-particle emission spectroscopy. The resonance scattering occurs due to the presence of a quasibound level of the formed nucleus, which is coupled to the scattering state of the decaying system. Thus, the asymptotic overlap integral becomes the wave function of relative motion of the fragments at large r values [34]: $I_n^k(r)\rightarrow u_n^0(r)$, $u_n^k(r)\rightarrow u_n^{o.b.}(r)$. The corresponding one-body width becomes

$$\Gamma_n^{o.b.}=2\pi\left|\frac{\int_{r_{\rm min}}^{r_{\rm max}}u_n^0(r)u_n^0(r)dr}{\int_{r_{\rm min}}^{r_{\rm max}}u_n^0(r)u_n^{o.b.}(r)dr}\right|^2, \quad (6)$$

TABLE I. Updated values [phenomenological, microscopic (SM), and macroscopic (one-body)] of parameters of the Brown relation [Eq. (8)] for AD half-lives. The AD data are taken from Refs. [5–20]. The Q_α values include available $Q_\alpha^{\rm exp}$ values plus calculated values from Eq. (11).

Fit of	Z,N	A	B	rms
Experim.	e-e	9.893	53.194	0.311
Data	o-e = e-o	9.424	50.014	0.448
($T_\alpha^{f\,\rm exp}$, $Q_\alpha^{\rm exp}$)	o-o	9.157	48.301	0.455
Shell model	e-e	10.5910	56.6181	0.0466
Calc.	o-e = e-o	10.1457	52.3859	0.1606
($T_\alpha^{f\,\rm SM}$, Q_α)	o-o	10.2964	53.7967	0.0779
One body	e-e	9.5520	52.5211	0.0300
Calc.	o-e = e-o	9.7424	52.5919	0.1999
($T_\alpha^{f\,o.b.}$, Q_α)	o-o	9.8662	53.099	0.1006

and the one-body resonance half-life is

$$T_n^{\rm res}=(\hbar\ln 2)/\Gamma_n^{o.b.}. \quad (7)$$

C. Systematics of AD half-lives: Empirical relationships

The first correlation between the α-half-time T_α and the emission energy Q_α type was observed by Geiger and Nuttall [59], who found that log T_α depends linearly on $Q_\alpha^{-1/2}$. Various generalizations of the Geiger-Nuttall law [38,60] systematically share this dependence. This is not surprising, because it originates from the common quantum penetration penetrability that depends linearly on $Q_\alpha^{-1/2}$. Brown [61] considered a modified Geiger-Nuttall law by an interpolation between $Q_\alpha^{-1/2}$ and the $Z_dQ_\alpha^{-1/2}$ dependence ($Z_d=Z-2$) and determined that the best representation of data is achieved by the linear dependence of the log T_α on $Z_d^{0.6}Q_\alpha^{-1/2}$ quantity. Including similar (Z,N) parity varying hindrance terms as in Refs. [34–38] proved the Brown formula to be an extremely powerful tool for describing the α-decay properties of SHN [50–54]. The Brown fit formula for the AD half-lives is taken in the form

$$\log_{10}T_\alpha({\rm sec})=AZ_d^{0.6}Q_\alpha^{-1/2}-B,\ {\rm rms}, \quad (8)$$

where A and B are the fit parameters, rms is the root mean square error, and T_α represents the fitted values of $T_\alpha^{\rm exp}$, $T_\alpha^{\rm SM}$, and $T_\alpha^{o.b.}$ for different (Z,N) parities (see Table I).

Recently, a fitting scheme leading to the modified Brown formula was proposed [38]:

$$\log_{10}T_\alpha^{mB1}=aZ_d^bQ_\alpha^{-1/2}+c+h_{Z,N}^{mB1},\quad {\rm rms}=0.3972, \quad (9)$$

where a, b, and c are parameters and $h_{Z,N}^{mB1}$ are even-odd corrections for each (Z,N) parity: $a=13.0705$, $b=0.5182$, $c=-47.8867$, and $h_{Z,N}^{mB1}=0$ ($Z=e,N=e$); 0.4666 ($Z=e,N=o$); 0.6001 ($Z=o,N=e$); 0.8200 ($Z=o,N=o$). The parameters of the empirical formulas [60,61] are usually established by fitting a large amount of data, which is subjected to significant errors and spread over regions of nuclide chart with different properties [5–20].

D. Spontaneous fission half-lives

Following Ref. [48], the SF half-life is expressed as

$$\log_{10} T_{\rm SF}(s) = 1146.44 - 75.3153X + 1.63792X^2 - 0.0119827X^3 + B_f(7.23613 - 0.0947022X) + h_{e\text{-}o}, \quad (10)$$

where $X = Z^2/A$, B_f is the SF [49], and $h_{e\text{-}o}$ are new even-odd corrections [51]: $h_{e\text{-}o} = 0$ for ($Z = e$, $N = e$), 2.007 for ($Z = e$, $N = o$), 2.822 for ($Z = o$, $N = e$), and 3.357 for ($Z = o$, $N = o$).

III. RESULTS AND DISCUSSION

A. Q_α-value estimates

For unknown nuclei around ^{270}Hs we perform AD energy predictions using prescriptions [46] and measured values (Q_1) in neighboring isobars ($A_1 = A_2$):

$$Q_2 = Q_1 - (\beta_2 - \beta_1)[(2/3)a_c A^{2/3}(\beta + 2) + 8a_{\rm sym}\beta] \quad (11)$$

with $\beta = (N - Z)/A$ denoting the isospin asymmetry, $Z = A(1 - \beta)/2$, $\beta = (\beta_1 + \beta_2)/2$, and $a_c = 0.71$. The mass dependence of the symmetry energy coefficient is given as $a_{\rm sym} = c_{\rm sym}(1 + kA^{-1/3})^{-1}$, where $c_{\rm sym}$ is the volume symmetry energy coefficient of the nuclei and k is the ratio of the surface symmetry coefficient to the volume symmetry coefficient. Here $c_{\rm sym} = 31.1$ and $k = 2.31$ are used without including the uncertainty. The decay energy used in Eq. (5) relations is

$$Q_\alpha({\rm MeV}) = A_p E_\alpha/A_d + \left(6.53Z_d^{7/5} - 8.0Z_d^{2/5}\right)10^{-5}, \quad (12)$$

where A_p and A_d are the mass numbers of the parent and daughter nuclei, E_α is the kinetic energy of α particle, and the second term is the screening correction. The experimental and calculated Q_α values in this work are presented in Fig. 1

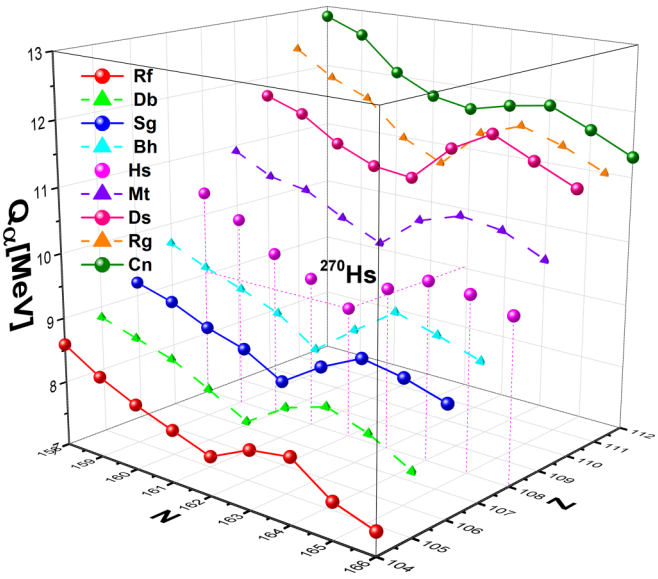

FIG. 1. The measured [5–20] (for 30 nuclei) and the calculated [46] from Eq. (11) (for 51 nuclei), Q_α values of the nuclei with Z=104–112 and N=158–166 as a function of Z and N.

and Table II. Calculated values are used for many neutron-deficient isotopes of Cn, Rg, Ds, and Mt (see also Table II). Once the parent or daughter nuclei have neutron or proton magic numbers (Figs. 1 and 2) the behavior of the Q_α value is dramatically changed. Thus, the irregular behavior of Q_α value confirms the existence of the magic shells. The Q_α values in Fig. 1 present a linear decreasing trend for $N = 158$–162 and $N = 164$–166 and an increasing trend for $N = 162$–164. Such a complicated trend was attributed [46] to the large symmetry energy that lowers the Q_α value at the magic shells. In Fig. 1, we can see an increasing trend of Q_α value with increasing Z. At ^{270}Hs the Q_α values markedly decrease since the nuclear binding energy increases strongly, and these give rise to an increased stability and half-life.

B. Ground-state–ground-state AD half-lives

The α-decay half-life estimates are obtained by using in Eq. (8) the parameters listed in Table I. These parameters are derived from the fit of experimental and calculated (SM and one-body) AD half-lives. The resulted AD half-lives and rms values are shown in Fig. 2 and Table II. The large rms value for experimental AD half-lives (Table I) denotes large uncertainties in measured half-lives and decay energies for known SHN. However, for the same decay energies the rms values for the SM and one-body half-lives are considerably smaller than for experimental data. In other words, the errors due to model approximations are small. If comparing in Table II the results of different approximations for AD half-lives one may conclude the following: (i) similar values for $T_\alpha^{f\rm SM}$ and $T_\alpha^{f\rm exp}$; (ii) two distinct relations [Eqs. (10) and (11)] with parameters extracted from the fit of the available experimental data for SHN give practically the same results for AD half-lives and rms values: $T_\alpha \approx T_\alpha^{mB1}$; (iii) the ratio $T_\alpha^{f\rm res}/T_\alpha^{f\rm SM} \approx 10^{-2}$ is a measure of the contribution of all the structure effects to AD; and (iv) the values $T_\alpha^{f\rm SM}$ are in good accordance with available experimental values $T_\alpha^{\rm exp}$.

One can see that the values T_α for the even-even nuclei are always smaller than those corresponding to the even-odd, odd-even, and odd-odd neighbors. Notice that by successive α decays the nuclear system becomes more stable. An example is the α-decay chain ^{274}Ds $\rightarrow$ ^{270}Hs $\rightarrow$ ^{266}Sg (see Table II), where the corresponding values T_α in the above α-decay chain increase: $T_\alpha(^{274}{\rm Ds}) < T_\alpha(^{270}{\rm Hs}) < T_\alpha(^{266}{\rm Sg})$.

We note that the parameter $h_{Z,N}^{mB1}$ in Eq. (9), which enters in the modified Brown formula proposed in Ref. [38], corrects in an average way the discrepancies between experimental and calculated α lifetimes for odd-odd nuclei. However, the discrepancies between experimental and calculated data for odd-even or even-odd nuclei still remain; see Table II. This is because the experimental rms values are quite large for all available data; see the last column in Table I. The errors come from inaccurate Q_α measurements. The values of ΔQ_α are quite large, in the range $\pm$(20–160) keV; see Ref. [18]. The largest experimental errors correspond to odd-mass nuclei; see Ref. [18]. However, for odd-odd nuclei, the experimental errors are smaller, resulting in a good agreement between theoretical and experimental data in Table II.

TABLE II. Experimental and calculated total α half-lives for ground-state–ground-state α transitions for the SHN around ^{270}Hs.

Nucleus	Q_α (MeV)	$T^{f\text{res}}$ (s)	$T^{f\text{SM}}$ (s)	$T^{f\text{exp}}$ (s)	T^{mB_1} (s)	T^{exp} (s)	$T^{f\text{res}}/T^{f\text{SM}}$	$T^{f\text{res}}/T^{f\text{exp}}$
^{262}Rf	8.490[a]	0.479×10^{-1}	0.699×10^{1}	0.133×10^{2}	0.187×10^{2}	0.287×10^{3}	0.684×10^{-2}	0.359×10^{-2}
^{263}Rf	8.250[a]	0.240×10^{1}	0.283×10^{3}	0.295×10^{3}	0.278×10^{3}	0.220×10^{4}	0.848×10^{-2}	0.812×10^{-2}
^{264}Rf	8.000	0.165×10^{1}	0.371×10^{3}	0.569×10^{3}	0.558×10^{3}		0.444×10^{-2}	0.290×10^{-2}
^{265}Rf	7.800	0.756×10^{2}	0.107×10^{5}	0.901×10^{4}	0.716×10^{4}		0.704×10^{-2}	0.839×10^{-2}
^{266}Rf	7.600	0.379×10^{2}	0.125×10^{5}	0.159×10^{5}	0.114×10^{5}		0.303×10^{-2}	0.239×10^{-2}
^{267}Rf	7.900	0.342×10^{2}	0.466×10^{4}	0.411×10^{4}	0.340×10^{4}		0.734×10^{-2}	0.833×10^{-2}
^{268}Rf	8.000	0.165×10^{1}	0.371×10^{3}	0.569×10^{3}	0.558×10^{3}		0.444×10^{-2}	0.290×10^{-2}
^{269}Rf	7.870	0.433×10^{2}	0.598×10^{4}	0.520×10^{4}	0.424×10^{4}		0.725×10^{-2}	0.834×10^{-2}
^{270}Rf	7.667	0.220×10^{2}	0.682×10^{4}	0.892×10^{4}	0.674×10^{4}		0.323×10^{-2}	0.247×10^{-2}
^{263}Db	8.830[a]	0.852×10^{-1}	0.827×10^{1}	0.105×10^{2}	0.146×10^{2}	0.783×10^{2}	0.103×10^{-1}	0.810×10^{-2}
^{264}Db	8.660	0.384×10^{0}	0.706×10^{2}	0.589×10^{2}	0.715×10^{2}		0.545×10^{-2}	0.653×10^{-2}
^{265}Db	8.500	0.825×10^{0}	0.904×10^{2}	0.996×10^{2}	0.123×10^{3}		0.912×10^{-2}	0.828×10^{-2}
^{266}Db	8.210	0.100×10^{2}	0.222×10^{4}	0.131×10^{4}	0.148×10^{4}		0.453×10^{-2}	0.768×10^{-2}
^{267}Db	7.900	0.730×10^{2}	0.102×10^{5}	0.845×10^{4}	0.834×10^{4}		0.716×10^{-2}	0.864×10^{-2}
^{268}Db	8.300	0.512×10^{1}	0.109×10^{4}	0.690×10^{3}	0.792×10^{3}		0.471×10^{-2}	0.742×10^{-2}
^{269}Db	8.500	0.825×10^{0}	0.904×10^{2}	0.996×10^{2}	0.123×10^{3}		0.912×10^{-2}	0.828×10^{-2}
^{270}Db	8.300[a]	0.512×10^{1}	0.109×10^{4}	0.690×10^{3}	0.792×10^{3}	0.477×10^{4}	0.471×10^{-2}	0.742×10^{-2}
^{271}Db	8.265	0.450×10^{1}	0.541×10^{3}	0.536×10^{3}	0.608×10^{3}		0.833×10^{-2}	0.841×10^{-2}
^{264}Sg	9.210	0.175×10^{-2}	0.166×10^{0}	0.377×10^{0}	0.623×10^{0}		0.106×10^{-1}	0.465×10^{-2}
^{265}Sg	9.050[a]	0.407×10^{-1}	0.374×10^{1}	0.492×10^{1}	0.478×10^{1}	0.800×10^{1}	0.109×10^{-1}	0.827×10^{-2}
^{266}Sg	9.020	0.579×10^{-2}	0.634×10^{0}	0.134×10^{1}	0.196×10^{1}		0.914×10^{-2}	0.433×10^{-2}
^{267}Sg	8.630[a]	0.683×10^{0}	0.730×10^{2}	0.804×10^{2}	0.676×10^{2}	0.494×10^{3}	0.936×10^{-2}	0.850×10^{-2}
^{268}Sg	8.300	0.772×10^{0}	0.153×10^{3}	0.240×10^{3}	0.213×10^{3}		0.503×10^{-2}	0.322×10^{-2}
^{269}Sg	8.700[a]	0.421×10^{0}	0.438×10^{2}	0.498×10^{2}	0.429×10^{2}	0.186×10^{3}	0.960×10^{-2}	0.846×10^{-2}
^{270}Sg	9.000	0.658×10^{-2}	0.731×10^{0}	0.153×10^{1}	0.221×10^{1}		0.900×10^{-2}	0.429×10^{-2}
^{271}Sg	8.890[a]	0.116×10^{0}	0.113×10^{2}	0.139×10^{2}	0.128×10^{2}	0.214×10^{3}	0.103×10^{-1}	0.835×10^{-2}
^{272}Sg	8.700	0.473×10^{-1}	0.668×10^{1}	0.124×10^{2}	0.146×10^{2}		0.708×10^{-2}	0.381×10^{-2}
^{265}Bh	9.680[a]	0.165×10^{-2}	0.126×10^{0}	0.201×10^{0}	0.287×10^{0}	0.119×10^{1}	0.131×10^{-1}	0.823×10^{-2}
^{266}Bh	9.430[a]	0.101×10^{-1}	0.147×10^{1}	0.176×10^{1}	0.195×10^{1}	0.250×10^{1}	0.688×10^{-2}	0.574×10^{-2}
^{267}Bh	9.230[a]	0.258×10^{-1}	0.228×10^{1}	0.306×10^{1}	0.379×10^{1}	0.220×10^{2}	0.113×10^{-1}	0.845×10^{-2}
^{268}Bh	9.000	0.160×10^{0}	0.272×10^{2}	0.243×10^{2}	0.253×10^{2}		0.589×10^{-2}	0.659×10^{-2}
^{269}Bh	8.600	0.173×10^{1}	0.192×10^{3}	0.196×10^{3}	0.196×10^{3}		0.903×10^{-2}	0.881×10^{-2}
^{270}Bh	9.060[a]	0.108×10^{0}	0.179×10^{2}	0.167×10^{2}	0.175×10^{2}	0.228×10^{3}	0.603×10^{-2}	0.646×10^{-2}
^{271}Bh	9.490[a]	0.515×10^{-2}	0.417×10^{0}	0.620×10^{0}	0.835×10^{0}	0.150×10^{1}	0.123×10^{-1}	0.832×10^{-2}
^{272}Bh	9.310[a]	0.215×10^{-1}	0.325×10^{1}	0.360×10^{1}	0.392×10^{1}	0.880×10^{1}	0.660×10^{-2}	0.596×10^{-2}
^{273}Bh	9.100	0.594×10^{-1}	0.548×10^{1}	0.697×10^{1}	0.827×10^{1}		0.108×10^{-1}	0.852×10^{-2}
^{266}Hs	10.346[a]	0.101×10^{-4}	0.494×10^{-3}	0.151×10^{-2}	0.360×10^{-2}	0.441×10^{-2}	0.204×10^{-1}	0.669×10^{-2}
^{267}Hs	10.076[a]	0.333×10^{-3}	0.229×10^{-1}	0.401×10^{-1}	0.422×10^{-1}	0.550×10^{1}	0.145×10^{-1}	0.830×10^{-2}
^{268}Hs	9.623[a]	0.560×10^{-3}	0.447×10^{-1}	0.106×10^{0}	0.168×10^{0}	0.142×10^{1}	0.125×10^{-1}	0.526×10^{-2}
^{269}Hs	9.370[a]	0.214×10^{-1}	0.184×10^{1}	0.247×10^{1}	0.209×10^{1}	0.270×10^{2}	0.116×10^{-1}	0.866×10^{-2}
^{270}Hs	9.050[a]	0.189×10^{-1}	0.232×10^{1}	0.444×10^{1}	0.486×10^{1}	0.360×10^{1}	0.816×10^{-2}	0.426×10^{-2}
^{271}Hs	9.510[a]	0.903×10^{-2}	0.744×10^{0}	0.105×10^{1}	0.932×10^{0}	0.400×10^{1}	0.122×10^{-1}	0.858×10^{-2}
^{272}Hs	9.780	0.225×10^{-3}	0.161×10^{-1}	0.406×10^{-1}	0.703×10^{-1}		0.140×10^{-1}	0.556×10^{-2}
^{273}Hs	9.730[a]	0.242×10^{-2}	0.186×10^{0}	0.286×10^{0}	0.271×10^{0}	0.760×10^{0}	0.130×10^{-1}	0.847×10^{-2}
^{274}Hs	9.570	0.766×10^{-3}	0.635×10^{-1}	0.148×10^{0}	0.226×10^{0}		0.121×10^{-1}	0.516×10^{-2}
^{267}Mt	10.900	0.819×10^{-5}	0.457×10^{-3}	0.100×10^{-2}	0.161×10^{-2}		0.179×10^{-1}	0.819×10^{-2}
^{268}Mt	10.600[a]	0.481×10^{-4}	0.505×10^{-2}	0.104×10^{-1}	0.112×10^{-1}	0.210×10^{-1}	0.953×10^{-2}	0.461×10^{-2}
^{269}Mt	10.500	0.640×10^{-4}	0.398×10^{-2}	0.764×10^{-2}	0.110×10^{-1}		0.161×10^{-1}	0.837×10^{-2}
^{270}Mt	10.180[a]	0.472×10^{-3}	0.563×10^{-1}	0.914×10^{-1}	0.925×10^{-1}	0.570×10^{0}	0.839×10^{-2}	0.517×10^{-2}
^{271}Mt	9.910	0.166×10^{-2}	0.123×10^{0}	0.191×10^{0}	0.232×10^{0}		0.135×10^{-1}	0.865×10^{-2}
^{272}Mt	10.400	0.140×10^{-3}	0.156×10^{-1}	0.289×10^{-1}	0.301×10^{-1}		0.898×10^{-2}	0.486×10^{-2}
^{273}Mt	10.600	0.378×10^{-4}	0.229×10^{-2}	0.455×10^{-2}	0.674×10^{-2}		0.165×10^{-1}	0.832×10^{-2}
^{274}Mt	10.510[a]	0.776×10^{-4}	0.836×10^{-2}	0.164×10^{-1}	0.174×10^{-1}	0.450×10^{0}	0.928×10^{-2}	0.472×10^{-2}
^{275}Mt	10.210[a]	0.306×10^{-3}	0.207×10^{-1}	0.360×10^{-1}	0.477×10^{-1}	0.970×10^{-2}	0.148×10^{-1}	0.850×10^{-2}
^{268}Ds	11.700	0.503×10^{-7}	0.126×10^{-5}	0.522×10^{-5}	0.187×10^{-4}		0.400×10^{-1}	0.965×10^{-2}
^{269}Ds	11.500[a]	0.852×10^{-6}	0.416×10^{-4}	0.104×10^{-3}	0.129×10^{-3}	0.230×10^{-3}	0.205×10^{-1}	0.819×10^{-2}

TABLE II. (*Continued.*)

Nucleus	Q_α (MeV)	$T^{f\text{res}}$ (s)	$T^{f\text{SM}}$ (s)	$T^{f\text{exp}}$ (s)	T^{mB_1} (s)	T^{exp} (s)	$T^{f\text{res}}/T^{f\text{SM}}$	$T^{f\text{res}}/T^{f\text{exp}}$
^{270}Ds	11.120[a]	0.727×10^{-6}	0.252×10^{-4}	0.883×10^{-4}	0.239×10^{-3}	0.160×10^{-3}	0.289×10^{-1}	0.823×10^{-2}
^{271}Ds	10.870[a]	0.179×10^{-4}	0.103×10^{-2}	0.212×10^{-2}	0.223×10^{-2}	0.210×10^{0}	0.174×10^{-1}	0.845×10^{-2}
^{272}Ds	10.800	0.347×10^{-5}	0.145×10^{-3}	0.463×10^{-3}	0.106×10^{-2}		0.239×10^{-1}	0.750×10^{-2}
^{273}Ds	11.370[a]	0.156×10^{-5}	0.789×10^{-4}	0.190×10^{-3}	0.227×10^{-3}	0.170×10^{-3}	0.198×10^{-1}	0.824×10^{-2}
^{274}Ds	11.700	0.503×10^{-7}	0.126×10^{-5}	0.522×10^{-5}	0.187×10^{-4}		0.400×10^{-1}	0.965×10^{-2}
^{275}Ds	11.400	0.136×10^{-5}	0.680×10^{-4}	0.165×10^{-3}	0.199×10^{-3}		0.200×10^{-1}	0.823×10^{-2}
^{276}Ds	11.110	0.763×10^{-6}	0.266×10^{-4}	0.929×10^{-4}	0.250×10^{-3}		0.287×10^{-1}	0.821×10^{-2}
^{269}Rg	12.063	0.125×10^{-6}	0.544×10^{-5}	0.152×10^{-4}	0.264×10^{-4}		0.230×10^{-1}	0.820×10^{-2}
^{270}Rg	11.686	0.807×10^{-6}	0.657×10^{-4}	0.206×10^{-3}	0.210×10^{-3}		0.123×10^{-1}	0.391×10^{-2}
^{271}Rg	11.439	0.209×10^{-5}	0.106×10^{-3}	0.248×10^{-3}	0.368×10^{-3}		0.198×10^{-1}	0.845×10^{-2}
^{272}Rg	11.197[a]	0.828×10^{-5}	0.768×10^{-3}	0.188×10^{-2}	0.180×10^{-2}	0.200×10^{-2}	0.108×10^{-1}	0.441×10^{-2}
^{273}Rg	10.900	0.290×10^{-4}	0.169×10^{-2}	0.333×10^{-2}	0.430×10^{-2}		0.172×10^{-1}	0.870×10^{-2}
^{274}Rg	11.480[a]	0.211×10^{-5}	0.182×10^{-3}	0.514×10^{-3}	0.511×10^{-3}	0.640×10^{-2}	0.116×10^{-1}	0.411×10^{-2}
^{275}Rg	11.700	0.626×10^{-6}	0.297×10^{-4}	0.751×10^{-4}	0.119×10^{-3}		0.211×10^{-1}	0.834×10^{-2}
^{276}Rg	11.500	0.192×10^{-5}	0.164×10^{-3}	0.470×10^{-3}	0.468×10^{-3}		0.117×10^{-1}	0.409×10^{-2}
^{277}Rg	11.200	0.656×10^{-5}	0.353×10^{-3}	0.766×10^{-3}	0.107×10^{-2}		0.186×10^{-1}	0.856×10^{-2}
^{270}Cn	12.241	0.159×10^{-7}	0.337×10^{-6}	0.147×10^{-5}	0.514×10^{-5}		0.471×10^{-1}	0.108×10^{-1}
^{271}Cn	11.997	0.303×10^{-6}	0.137×10^{-4}	0.358×10^{-4}	0.405×10^{-4}		0.222×10^{-1}	0.846×10^{-2}
^{272}Cn	11.759	0.127×10^{-6}	0.348×10^{-5}	0.133×10^{-4}	0.373×10^{-4}		0.366×10^{-1}	0.957×10^{-2}
^{273}Cn	11.465	0.342×10^{-5}	0.176×10^{-3}	0.394×10^{-3}	0.389×10^{-3}		0.195×10^{-1}	0.869×10^{-2}
^{274}Cn	11.220	0.153×10^{-5}	0.563×10^{-4}	0.185×10^{-3}	0.397×10^{-3}		0.271×10^{-1}	0.826×10^{-2}
^{275}Cn	11.750	0.915×10^{-6}	0.438×10^{-4}	0.107×10^{-3}	0.114×10^{-3}		0.209×10^{-1}	0.856×10^{-2}
^{276}Cn	11.900	0.684×10^{-7}	0.173×10^{-5}	0.689×10^{-5}	0.206×10^{-4}		0.395×10^{-1}	0.992×10^{-2}
^{277}Cn	11.620[a]	0.166×10^{-5}	0.820×10^{-4}	0.192×10^{-3}	0.198×10^{-3}	0.110×10^{-2}	0.202×10^{-1}	0.862×10^{-2}
^{278}Cn	11.310	0.995×10^{-6}	0.349×10^{-4}	0.117×10^{-3}	0.265×10^{-3}		0.285×10^{-1}	0.847×10^{-2}

[a]measured Q_α^{exp} values.

Figure 4 reveals a main SF channel in $N = 160$ ($Z =$ even) sequence, and a main α-decay channel in $N = 164$ sequence. Comparing the results from Figs. 2 and 4 we may conclude that the SHN from unstable configurations undergo spontaneous α decay or SF until the nuclear stability is reached. Our results for the decay properties of SHN around ^{270}Ds are in good agreement with existing data. The α-decay half-life (Fig. 3) varies approximately with $Q_\alpha^{1/2}$ and shows an irregular trend at the magic shells $Z = 108$ and $N = 162$.

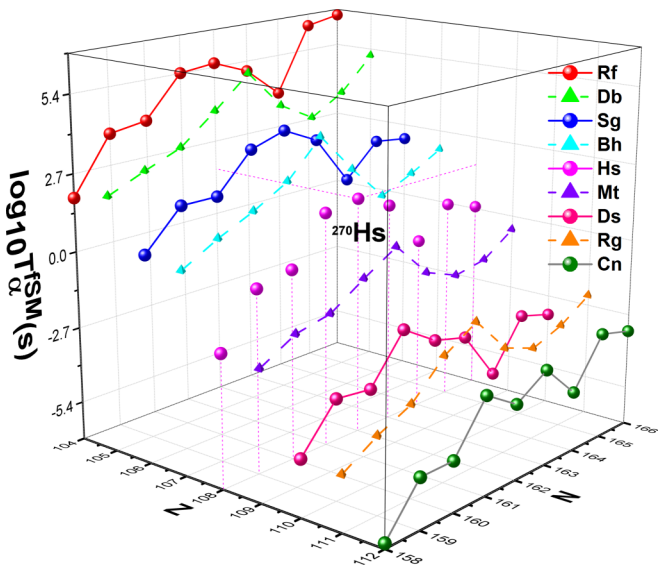

FIG. 2. The α-decay half-lives, $T_\alpha^{f\text{SM}}$ given by Eq. (8), with the SM parameters resulted from the fit of the SM α half-lives, as a function of Z and N.

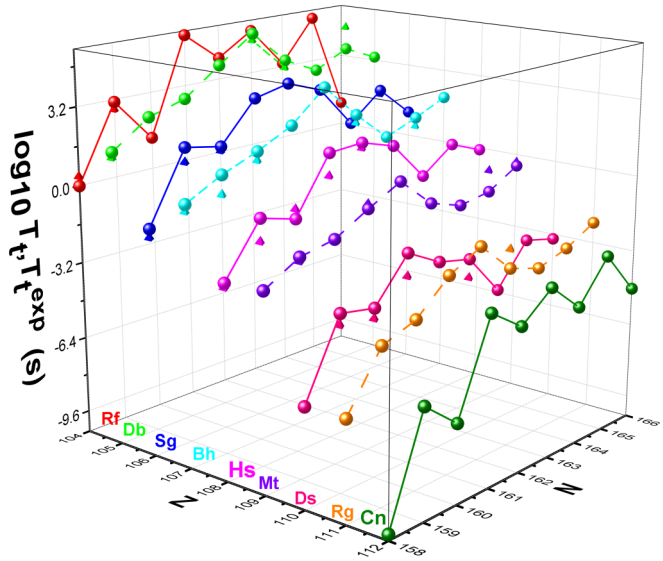

FIG. 3. The total experimental (triangle) and calculated from $T_\alpha^{f\text{SM}}$ and T_{SF} values (sphere) half-lives of nuclei with $Z = 104$–112 and $N = 158$–166, as a function of Z and N. The values of $T_\alpha^{f\text{SM}}$ are shown in Fig. 2 and Table II, while those of T_{SF} are given by Eq. (10).

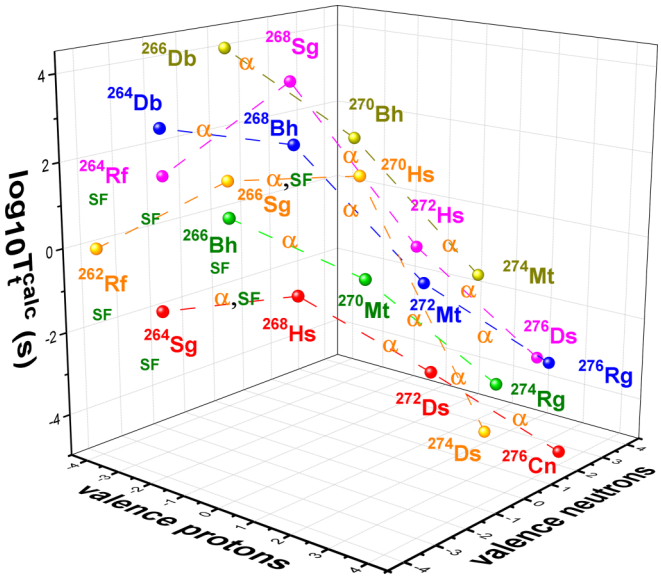

FIG. 4. The total half-lives of SHN with $Z = 104$–112 and $N = 158$–166 calculated from T_α^{fSM} and T_{SF} values as a function of the numbers of valence nucleons (holes) of the doubly magic core ^{270}Hs. The AD channels starting from parent nuclei with valence nucleons are always terminating at spontaneously fissioning nuclei with nucleon holes.

C. Total half-lives and branching ratios

The closed $Z = 108$ proton shell can be seen as a large gap between Hs and in isotopes Fig. 1. Hence, going from Hs to Ds isotopes, Q_α decreases, corresponding to an increase in T, reflecting enhanced stability for Hs isotopes ($Z = 108$). In addition, the shell closure at $N = 162$ also enhances stability of isotopes leading to a local minimum at $N = 162$. The total half-life is represented in Figs. 4 and 5 as a function of the numbers of valence nucleons and as a function of Z and N, respectively. In general, the region around the shell closures of ^{270}Hs forms a landscape of α emitters surrounded by spontaneously fissioning nuclei, as shown in Fig. 5. Figure 5 includes our predicted decay properties for 51 nuclei for which there are no available experimental data. The dominant decay mode of ^{270}Hs as well as ^{268}Hs and ^{272}Hs is AD. While ^{270}Hs has a half-life of the order of a few seconds, other isotopes should decay within a half-life shorter than 1 s as a result of stabilization effects of the $N = 162$ closed shell. The daughter nuclides ^{266}Sg and ^{262}Rf decay via SF, which is more probable than AD. For even-odd nuclei, similar calculations can be done resulting in AD as dominant decay mode for ^{269}Hs and ^{271}Hs as well as for their daughters ^{265}Sg and ^{267}Sg. For ^{268}Bh, ^{268}Sg, and ^{268}Hs, the partial half-lives for AD and SF are comparable and hence there will be almost equal AD and SF branching ratios. AD dominates in nuclei over closed shells

Cn Z=112	270 12.834 0.0565 ns 0.00;1.00	271 12.598 1.13 µs 0.11; 0.89	272 12.058 0.0615 µs 0.01; 0.99	273 11.764 382 µs 0.76; 0.24	274 11.650 35.2 µs 0.43; 0.57	275 11.800 424 µs 1.00; 0.00	276 11.900 2.4 µs 0.93; 0.07	277 11.620 1.02 ms 0.99; 0.01	278 11.310 14.6 µs 0.03; 0.97
Rg Z=111	269 12.373 0.464 µs 0.03; 0.97	270 11.986 79.8 µs 0.92;0.08	271 11.740 0.25 ms 0.81; 0.19	272 11.197 4.49 ms 1.00;0.00	273 10.900 22.7 ms 0.98;0.02	274 11.480 1.04 ms 1.00; 0.00	275 11.700 0.374 ms 1.00; 0.00	276 11.500 0.943 ms 1.00;0.00	277 11.200 4.56 ms 0.97;0.03
Ds Z=110	268 11.700 0.416 µs 0.02; 0.98	269 11.500 0.515 ms 0.96; 0.04	270 11.120 0.266 ms 0.72; 0.28	271 10.870 14.4 ms 1.00;0.00	272 10.800 2.23 ms 1.00; 0.00	273 11.370 1.04 ms 1.00; 0.00	274 11.700 17.4 µs 1.00; 0.00	275 11.400 0.891 ms 1.00; 0.00	276 11.110 0.388 ms 0.99; 0.01
Mt Z=109	267 10.900 4.54 ms **0.71; 0.29**	268 10.600 31.7 ms **0.99; 0.01**	269 10.500 58 ms **0.99; 0.01**	270 10.180 0.371 s **1.00; 0.00**	271 9.910 1.96 s **1.00; 0.00**	272 10.400 0.101 s **1.00; 0.00**	273 10.600 33.4 ms **1.00; 0.00**	274 10.510 53.5 ms **1.00; 0.00**	275 10.210 0.315 s **1.00; 0.00**
Hs Z=108	266 10.346 3.53 ms 0.43;0.57	267 10.037 0.451 s 0.99; 0.01	268 9.623 0.165 s 0.20; 0.80	269 9.370 32 s 0.99; 0.01	270 9.050 37.5 s 0.80; 0.20	271 9.510 12.7 s 1.00; 0.00	272 9.780 0.29 s 1.00; 0.00	273 9.730 3.07 s 1.00; 0.00	274 9.570 0.821 s 0.70; 0.30
Bh Z=107	265 9.680 1.78 s 0.84; 0.16	266 9.430 10.7 s 1.00;0.00	267 9.230 40.6 s 0.99;0.01	268 9.000 3.48 min 1.00;0.00	269 8.600 63.5 min 1.00; 0.00	270 9.060 2.26 min 1.00; 0.00	271 9.490 7.22 s 1.00;0.00	272 9.310 24.1 s 1.00; 0.00	273 9.100 96.3 s 0.96; 0.04
Sg Z=106	264 9.210 84.7 ms 0.03; 0.97	265 9.050 65.1 s 0.93; 0.07	266 8.800 32.2 s 0.47;0.53	267 8.630 24.33 min 1.00; 0.00	268 8.300 51.66 min 0.86; 0.14	269 8.700 14.5 min 1.00; 0.00	270 9.000 15.2 s 1.00;0.00	271 8.890 3.61 min 1.00;0.00	272 8.700 11.6 s 0.08; 0.92
Db Z=105	263 8.830 46 s 0.28; 0.72	264 8.660 9.21 min 0.95; 0.05	265 8.500 25.5 min 0.81;0.19	266 8.210 5.36 h 1.00;0.00	267 7.900 62.22 h 0.95; 0.05	268 8.300 2.6 h 1.00; 0.00	269 8.500 31.16 min 1.00; 0.00	270 8.300 2.58h 0.99; 0.01	271 7.960 36 min 0.02; 0.98
Rf Z=104	262 8.590 0.961 s 0.01; 0.99	263 8.250 20.66 min 0.20; 0.80	264 8.000 19.6 s 0.00; 1.00	265 7.800 58.61 h 0.82; 0.18	266 7.600 3.52 h 0.04; 0.96	267 7.900 30.27 h 0.99; 0.01	268 8.000 36.83 min 0.23; 0.77	269 7.564 37.5 h 0.07; 0.93	270 7.361 9.36 s 0.00; 1.00
N	**158**	**159**	**160**	**161**	**162**	**163**	**164**	**165**	**166**

FIG. 5. The summary of predicted decay properties of 81 SHN with $Z = 104$–112 and $N = 158$–166. For each nuclide the mass number $A = Z + N$, Q_α value for the ground-state–ground-state decay, the total half-life T_t (resulted from T_α^{fSM} and T_{SF} values), and the branching ratios b_α and b_{SF} for α decay and SF are shown. The nuclei colored in yellow are prominent α emitters ($b_\alpha > b_{SF}$), while the spontaneously fissioning nuclei are colored in green ($b_\alpha < b_{SF}$).

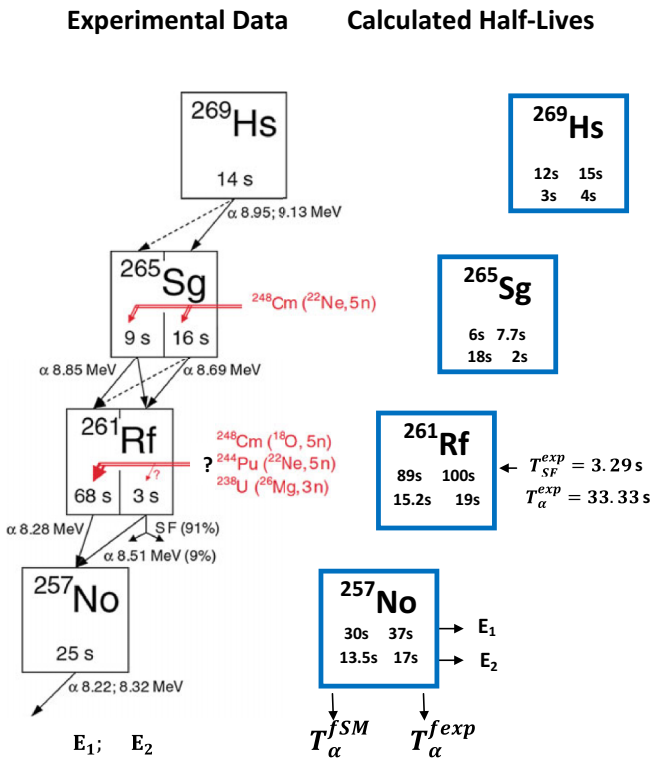

FIG. 6. Experimental [17,67] and presently calculated $T_\alpha^{f\mathrm{SM}}$ AD half-lives for transitions from the ground to excited states in the α chain starting from ^{269}Hs.

$Z > 108$, $N > 162$ (with valence nucleons and α particles) (^{274}Ds $= {}^{270}$Hs $+\alpha$), while SF dominates in nuclei below the closed shells (^{266}Sg $= {}^{270}$Hs $-\alpha$) (with valence holes and α particles). From Figs. 3–5 and Table II we can see that nuclei from this studied region are typically unstable with respect to both AD and SF. Strong competition between AD and SF is observed in even-even nuclei. Also, T_{SF} increases considerably due to the effect of unpaired nucleons and T_α is much less sensitive to the unpaired nucleons. We found in the literature only a few predictions for the Q values in the region of nuclei with $Z = 104$–112 and $N = 158$–166. We compare the results obtained from Eq. (11) to those from the work by Baran *et al.* [62]. Our predictions for Q_α values are close to the predictions of Ref. [62], excepting ^{266}Sg. It is worth mentioning that Baran *et al.* [62] predicted only the spontaneous fission for the nuclei ^{262}Rf, ^{266}Hs, ^{270}Hs, and ^{270}Ds, while we predicted only the α-decay mode for ^{270}Hs and ^{270}Ds. For ^{266}Hs we predict the branching ratios $b_\alpha = 0.43$ and $b_{\mathrm{SF}} = 0.57$, while the experimental branching ratio estimations are $b_\alpha = 0.68$ and $b_{\mathrm{SF}} = 0.32$. These values indicate a strong competition between α decay and spontaneous fission.

D. Ground-state–excited-states AD half-lives

The investigation of the decay properties of the Hs isotopes and their daughter nuclei was performed for the first time in Ref. [63]. We estimate the AD half-lives for transitions between the ground state of the parent nucleus and excited states of the daughter nuclei by using the approximations based on Eq. (8) and Table I and making use of two simplifying assumptions [64]: (i) the α-formation amplitude [Eq. (3)] for the excited state is the same as that in the ground state, and (ii) the shapes and deformations of the parent and daughter nuclei are the same. We can observe in Fig. 6 a good accordance between calculated and experimental half-lives in spite of above mentioned assumptions. Recently [65,66], it was proven that the shell effects play a major role in the stability of ground and metastable states in SHN.

IV. CONCLUSIONS

The progress in studies of SHN is due to the exceptional role of fundamental measurements to understanding of nuclei at their limits of existence for mass, charge, excitation energy, and spin [5,68]. However, two major difficulties arise in studies of SHN. One is related to reaction mechanism for their production at very small cross sections and the other one to the study of their nuclear decay properties for extremely weak reaction channels. In this work we gave a systematic overview of the available experimental data and the calculated nuclear decay characteristics of nuclei around ^{270}Hs. New half-life predictions are made for 51 unknown nuclei from this region. The calculated ground-state–ground-state and ground-state–excited-state half-lives are in good agreement with existing data. In brief, we proved that it is possible to inter-relate most nuclear species on the reaction energies half-lives basis and to determine the regions of greater stability. Some of our results may help in synthesis and identification of new heaviest nuclei.

ACKNOWLEDGMENTS

We thank Prof. Yu. Ts. Oganessian, Prof. V. K. Utyonkov, Prof. G. Münzenberg, Prof. W. Scheid, Prof. A. Săndulescu, Prof. D. Mihalache, Prof. M. Mirea, and Prof. A. I. Budaca for many stimulating discussions. This work was supported by Project Nucleu No. PN 16 42 01 01.

[1] G. N. Flerov *et al.*, Proceedings of the International Conference on Heavy Ion Physics, Dubna, USSR, 1971, Joint Institute for Nuclear Research Report No. JINRD7-5769, 1971 (unpublished), p. 125.
[2] Y. T. Oganessian *et al.*, Nucl. Phys. A **239**, 157 (1975).
[3] G. Münzenberg *et al.*, Nucl. Instrum. Methods **161**, 65 (1979).
[4] L. P. Somerville, M. J. Nurmia, J. M. Nitschke, A. Ghiorso, E. K. Hulet, and R. W. Lougheed, Phys. Rev. C **31**, 1801 (1985).
[5] S. Hofmann and G. Münzenberg, Rev. Mod. Phys. **72**, 733 (2000).
[6] K. Morita *et al.*, J. Phys. Soc. Japan **73**, 2593 (2004).
[7] Y. T. Oganessian, V. K. Utyonkov, Y. V. Lobanov, F. S. Abdullin, A. N. Polyakov, R. N. Sagaidak, I. V. Shirokovsky, Y. S. Tsyganov, A. A. Voinov, G. G. Gulbekian, S. L. Bogomolov, B. N. Gikal, A. N. Mezentsev, S. Iliev, V. G. Subbotin, A. M. Sukhov, K. Subotic, V. I. Zagrebaev, G. K. Vostokin, M. G. Itkis,

K. J. Moody, J. B. Patin, D. A. Shaughnessy, M. A. Stoyer, N. J. Stoyer, P. A. Wilk, J. M. Kenneally, J. H. Landrum, J. F. Wild, and R. W. Lougheed, Phys. Rev. C **74**, 044602 (2006).
[8] Y. T. Oganessian, F. S. Abdullin, C. Alexander, J. Binder, R. A. Boll, S. N. Dmitriev, J. Ezold, K. Felker, J. M. Gostic, R. K. Grzywacz, J. H. Hamilton, R. A. Henderson, M. G. Itkis, K. Miernik, D. Miller, K. J. Moody, A. N. Polyakov, A. V. Ramayya, J. B. Roberto, M. A. Ryabinin, K. P. Rykaczewski, R. N. Sagaidak, D. A. Shaughnessy, I. V. Shirokovsky, M. V. Shumeiko, M. A. Stoyer, N. J. Stoyer, V. G. Subbotin, A. M. Sukhov, Y. S. Tsyganov, V. K. Utyonkov, A. A. Voinov, and G. K. Vostokin, Phys. Rev. C **87**, 054621 (2013).
[9] S. Hofmann *et al.*, Eur. Phys. J. A **10**, 5 (2001).
[10] J. Dvorak, W. Bruchle, M. Chelnokov, R. Dressler, C. E. Dullmann, K. Eberhardt, V. Gorshkov, E. Jager, R. Krcken, A. Kuznetsov, Y. Nagame, F. Nebel, Z. Novackova, Z. Qin, M. Schadel, B. Schausten, E. Schimpf, A. Semchenkov, P. Thorle, A. Turler, M. Wegrzecki, B. Wierczinski, A. Yakushev, and A. Yeremin, Phys. Rev. Lett. **97**, 242501 (2006).
[11] J. Dvorak, W. Bruchle, M. Chelnokov, C. E. Dullmann, Z. Dvorakova, K. Eberhardt, R. Eichler, E. Jager, R. Krucken, A. Kuznetsov, Y. Nagame, F. Nebel, K. Nishio, R. Perego, Z. Qin, M. Schadel, B. Schausten, E. Schimpf, R. Schuber, A. Semchenkov, P. Thorle, A. Turler, M. Wegrzecki, B. Wierczinski, A. Yakushev, and A. Yeremin, Phys. Rev. Lett. **100**, 132503 (2008).
[12] P. A. Ellison, K. E. Gregorich, J. S. Berryman, D. L. Bleuel, R. M. Clark, I. Dragojevic, J. Dvorak, P. Fallon, C. Fineman-Sotomayor, J. M. Gates, O. R. Gothe, I. Y. Lee, W. D. Loveland, J. P. McLaughlin, S. Paschalis, M. Petri, J. Qian, L. Stavsetra, M. Wiedeking, and H. Nitsche, Phys. Rev. Lett. **105**, 182701 (2010).
[13] R. Graeger, D. Ackermann, M. Chelnokov, V. Chepigin, C. E. Dullmann, J. Dvorak, J. Even, A. Gorshkov, F. P. Hessberger, D. Hild, A. Hubner, E. Jager, J. Khuyagbaatar, B. Kindler, J. V. Kratz, J. Krier, A. Kuznetsov, B. Lommel, K. Nishio, H. Nitsche, J. P. Omtvedt, O. Petrushkin, D. Rudolph, J. Runke, F. Samadani, M. Schadel, B. Schausten, A. Turler, A. Yakushev, and Q. Zhi, Phys. Rev. C **81**, 061601(R) (2010).
[14] H. Haba, D. Kaji, H. Kikunaga, Y. Kudou, K. Morimoto, K. Morita, K. Ozeki, T. Sumita, A. Yoneda, Y. Kasamatsu, Y. Komori, K. Ooe, and A. Shinohara, Phys. Rev. C **83**, 034602 (2011).
[15] A. Tuerler, Radiochim. Acta **100**, 75 (2012).
[16] Y. T. Oganessian, V. K. Utyonkov, F. S. Abdullin, S. N. Dmitriev, R. Graeger, R. A. Henderson, M. G. Itkis, Y. V. Lobanov, A. N. Mezentsev, K. J. Moody, S. L. Nelson, A. N. Polyakov, M. A. Ryabinin, R. N. Sagaidak, D. A. Shaughnessy, I. V. Shirokovsky, M. A. Stoyer, N. J. Stoyer, V. G. Subbotin, K. Subotic, A. M. Sukhov, Y. S. Tsyganov, A. Turler, A. A. Voinov, G. K. Vostokin, P. A. Wilk, and A. Yakushev, Phys. Rev. C **87**, 034605 (2013).
[17] J. H. Hamilton, S. Hofmann, and Y. T. Oganessian, Annu. Rev. Nucl. Part. Sci. **63**, 383 (2013).
[18] Y. T. Oganessian and V. K. Utyonkov, Nucl. Phys. A **944**, 62 (2015).
[19] V. K. Utyonkov, N. T. Brewer, Y. T. Oganessian, K. P. Rykaczewski, F. S. Abdullin, S. N. Dmitriev, R. K. Grzywacz, M. G. Itkis, K. Miernik, A. N. Polyakov, J. B. Roberto, R. N. Sagaidak, I. V. Shirokovsky, M. V. Shumeiko, Y. S. Tsyganov, A. A. Voinov, V. G. Subbotin, A. M. Sukhov, A. V. Sabelnikov, G. K. Vostokin, J. H. Hamilton, M. A. Stoyer, and S. Y. Strauss, Phys. Rev. C **92**, 034609 (2015).
[20] Chart of Nuclides, NNDC Brookhaven National Laboratory, sonzogni@bnl.gov.
[21] A. Sobiczewski *et al.*, Phys. Lett. **22**, 500 (1966).
[22] S. G. Nilsson *et al.*, Nucl. Phys. A **115**, 545 (1968).
[23] U. Mosel and W. Greiner, Z. Phys. **222**, 261 (1969).
[24] E. O. Fiset and J. R. Nix, Nucl. Phys. A **193**, 647 (1972).
[25] Z. Patyk and A. Sobiczewski, Nucl. Phys. A **533**, 132 (1991).
[26] R. Smolanczuk, J. Skalski, and A. Sobiczewski, Phys. Rev. C **52**, 1871 (1995).
[27] I. Muntian, Z. Patyk, and A. Sobiczewski, Phys. Rev. C **60**, 041302 (1999).
[28] I. Muntian, Z. Patyk, and A. Sobiczewski, Phys. Lett. B **500**, 241 (2001).
[29] A. Sobiczewski and K. Pomorski, Prog. Part. Nucl. Phys. **58**, 292 (2007).
[30] Y. Qian and Z. Ren, Phys. Rev. C **90**, 064308 (2014).
[31] Y. Qian and Z. Ren, Phys. Lett. B **738**, 87 (2014).
[32] B. Sahu and S. Bhoi, Phys. Rev. C **93**, 044301 (2016).
[33] C. Xu, X. Zhang, and Z. Ren, Nucl. Phys. A **898**, 24 (2013).
[34] I. Silisteanu and A. I. Budaca, At. Data Nucl. Data Tables **98**, 1096 (2012).
[35] A. I. Budaca and I. Silisteanu, Phys. Rev. C **88**, 044618 (2013).
[36] A. I. Budaca and I. Silisteanu, J. Phys.: Conf. Ser. **337**, 012022 (2012).
[37] A. I. Budaca and I. Silisteanu, J. Phys.: Conf. Ser. **413**, 012027 (2013).
[38] A. I. Budaca, R. Budaca, and I. Silisteanu, Nucl. Phys. A **951**, 60 (2016).
[39] I. Silisteanu, A. I. Budaca, and A. O. Silisteanu, Rom. J. Phys. **55**, 1088 (2010).
[40] I. Silisteanu and A. I. Budaca, Rom. J. Phys. **58**, 1198 (2013).
[41] S. P. Maydanyuk, P.-M. Zhang, and L.-P. Zou, Phys. Rev. C **93**, 014617 (2016).
[42] S. P. Maydanyuk, P.-M. Zang, and S. V. Belchikov, Nucl. Phys. A **940**, 89 (2015).
[43] V. Y. Denisov, O. I. Davidovskaya, and I. Y. Sedykh, Phys. Rev. C **92**, 014602 (2015).
[44] R. Budaca, A. Sandulescu, and M. Mirea, Mod. Phys. Lett. A **30**, 1550129 (2015).
[45] N. Wang, M. Liu, X. Wu, and J. Meng, Phys. Rev. C **93**, 014302 (2016).
[46] J. Dong, W. Zuo, and W. Scheid, Phys. Rev. Lett. **107**, 012501 (2011).
[47] P. Moller, J. Nix, and K. L. Kratz, At. Data Nucl. Data Tables **66**, 131 (1997).
[48] I. V. Karpov *et al.*, Int. J. Mod. Phys. E **21**, 1250013 (2012).
[49] P. Moller, A. J. Sierk, T. Ichikawa, A. Iwamoto, and M. Mumpower, Phys. Rev. C **91**, 024310 (2015).
[50] I. Silisteanu and C. I. Anghel, Rom. J. Phys. **59**, 724 (2014).
[51] I. Silisteanu and C. I. Anghel, Rom. J. Phys. **60**, 444 (2015).
[52] I. Silisteanu and C. I. Anghel, AIP Conf. Proc. **1694**, 020008 (2015).
[53] C. I. Anghel and A. O. Silisteanu, AIP Conf. Proc. **1694**, 020014 (2015).
[54] I. Silisteanu and C. I. Anghel, EPJ Web Conf. **107**, 07004 (2016).

[55] A. Sandulescu and I. Silisteanu, Nucl. Phys. A **272**, 148 (1976).
[56] I. Silisteanu and W. Scheid, Phys. Rev. C **51**, 2023 (1995).
[57] V. Ledoux *et al.*, J. Comp. App. Math. **228**, 197 (2009).
[58] V. L. Makarov *et al.*, J. Comp. App. Math. **250**, 39 (2013).
[59] H. Geiger and J. M. Nuttall, Philos. Mag. **22**, 613 (1911).
[60] V. E. Viola and G. T. Seaborg, J. Inorg. Nucl. Chem. **28**, 741 (1966).
[61] B. A. Brown, Phys. Rev. C **46**, 811 (1992).
[62] A. Baran, Z. Lojewski, K. Sieja, and M. Kowal, Phys. Rev. C **72**, 044310 (2005).
[63] J. Dvorak, Ph.D. thesis, Technische University at München, München, Germany, 2006 (unpublished).
[64] V. Y. Denisov and A. A. Khudenko, Phys. Rev. C **80**, 034603 (2009).
[65] D. Aranghel and A. Sandulescu, Rom. J. Phys. **60**, 147 (2015).
[66] D. Aranghel and A. Sandulescu, Rom. J. Phys. **60**, 1433 (2015).
[67] R. Graeger, Ph.D. thesis, Technical University, Faculty of Chemistry, München, München, Germany, 2010 (unpublished).
[68] Y. T. Oganessian, A. Sobiczewski, and G. M. Ter-Akopian, Phys. Scr. **92**, 023003 (2017).